Steady-state SR-EPG optimization of pseudo-steady-state sequences

Shaihan Malik[1] and Joseph V Hajnal[1]
[1]*Division of Imaging Sciences and Biomedical Engineering, Kings College London, London, London, United Kingdom*

Introduction RF field (B_1) variation at high field strengths (3T+) leads to spatially variable signal and tissue contrast, reducing both clinical and scientific utility of resulting images. By allowing independent modulation of the relative weighting of multiple transmit channels, parallel transmission (PTx) enables spatial and temporal modulation of the B_1 field, a feature which cannot be achieved using standard single channel transmit systems. These new degrees of freedom can be employed during MR imaging sequences in order to influence the resulting signal and contrast. In the simplest and most widely used approach, RF shimming [1], the B_1 field is spatially adapted and then held fixed for an entire imaging sequence. Another approach more commonly used in research applications is to optimise RF pulse waveforms themselves; in contrast to RF shimming this yields RF field patterns that change dynamically over durations of microseconds or milliseconds depending on the pulse. Rather than optimising field patterns as is the case with RF shimming, tailored RF pulse design seeks to optimize the resulting excited (or refocused) magnetization immediately after a given pulse, and pulses are usually treated in isolation from one another. Recently a third alternative, dynamic RF shimming was proposed, in which field patterns are changed on a pulse by pulse basis in order to influence the resulting signals arising from the sequence as a whole [2]. This method acknowledges the fact that resulting signals are influenced by the interaction between consecutive pulses and the NMR system: it is the signals themselves rather than fields or excited magnetization which are optimized, using a Spatially Resolved Extended Phase Graph (SR-EPG) model. The SR-EPG approach was demonstrated for the case of 3D TSE sequences [3,4] employing long trains of low refocusing flip angles. In such a sequence it is common for approximately 100 echoes to be collected in a single shot. In order to generate 3D high-resolution images, it is however necessary to collect a large number of shots. The SR-EPG framework considers signal evolution during an echo train, but in the original method the magnetization at the start was assumed to be in thermal equilibrium. This neglects the effect of incomplete (and spatially variable) recovery in a multi-shot sequence, resulting in suboptimal results. In this work the SR-EPG method is extended to optimize the steady-state arising from multiple shots, in contrast with the transient effect of only a single shot in isolation as in the original method.

Methods The SR-EPG framework allows the calculation of the echo amplitudes as a function of space and echo number, which we write as $S(\mathbf{r},n)=f(\boldsymbol{\theta}(\mathbf{r}),E_1(\mathbf{r}),E_2(\mathbf{r}))$ where $\boldsymbol{\theta}(\mathbf{r})=\{\theta_0(\mathbf{r}),\theta_1(\mathbf{r}),\ldots,\theta_n(\mathbf{r})\}$ is the set of flip angles used ($\theta_0(\mathbf{r})$ is the excitation pulse); $E_{1,2}(\mathbf{r})=\exp\{-ES/T_{1,2}(\mathbf{r})\}$ where ES is the echo spacing; and "*f*" represents use of the EPG algorithm [5]. The flip angles are written as functions of space such that $\boldsymbol{\theta}(\mathbf{r}) = \mathbf{A}\,\boldsymbol{\sigma}(\mathbf{r})$ where $\boldsymbol{\sigma}(\mathbf{r})$ contains the sensitivity of each element of the transmit array at location $\mathbf{r}$ and $\mathbf{A}_{ij}$ contains the complex drives applied to the j^{th} channel for the i^{th} pulse. In order to simulate a steady state, the EPG algorithm is used successively for a number of shots (Nshots). It is assumed that all remaining transverse magnetization is dephased between shots and that the only surviving state is the lowest order longitudinal state $Z_0(\mathbf{r})$, whose population increases with T_1 recovery between shots. The simulated echo amplitudes for the final simulated shot $S(\mathbf{r},n)$ are taken to reflect the steady-state, which is the case as long as Nshots is sufficiently large (Nshots=5 in this work). Optimized flip angles $\mathbf{A}$ are found by performing the minimization in Eq.1 using a stochastic non-linear optimization technique (Self Organizing Migratory Algorithm, SOMA, [6,7]). I_T is the target echo amplitude, β is a regularization parameter designed to limit RF power and λ is used to ensure that the phase of the echo amplitudes remains temporally stable to avoid image artifacts (it can be spatially variable). B_1 field data were obtained using the AFI sequence [8] in the brain of a healthy volunteer using a Philips 3T Achieva MRI system with an 8-channel PTx body coil [9]. The TSE sequence used non-selective RF pulses, TR=2500ms, ES=4.6ms and 100 echoes per shot. The base sequence depicted in Fig 1a employed a pseudo-steady-state (PSS) with relative echo amplitude of 0.5. The last 3 pulses in the train are designed to restore longitudinal magnetization for the next shot [10] using angles 59°, 113° and -90°. Subsequent optimizations used I_T=0.5 for all locations and echoes. In principle all 103 pulses could be independently optimised using SR-EPG, but to reduce complexity only the first 5 were optimized independently with the next 95 having a common RF field pattern as represented by the coloured rectangles on Fig. 1a. In the steady-state case the last 3 pulses were also optimized since they affect echo amplitudes in the *next* shot; for the transient case these are included in the sequence but are not optimized. In all cases the optimization neglected relaxation effects (i.e. T_1=T_2=∞) during each shot but for steady state optimization T_1 recovery was simulated between shots using a value representative of CSF (3 sec). Subsequently, full steady-state simulations were performed in order to assess the quality of all solutions for 3 different tissue types: CSF, gray matter (GM) and white matter (WM).

$$\min_{\mathbf{A}}\left\{\sum_{n,\mathbf{r}}\left(|S(\mathbf{r},n)|-I_T\right)^2+\lambda\sum_{n,\mathbf{r}}\left(\frac{\partial}{\partial n}\left(\arg\left(S(\mathbf{r},n)\right)\right)\right)^2+\beta\|\mathbf{A}\|_F^2\right\} \quad Eq.1$$

Fig 1

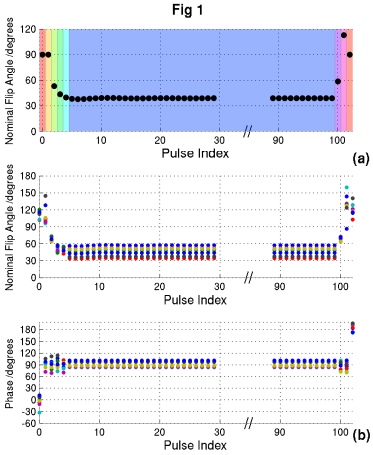

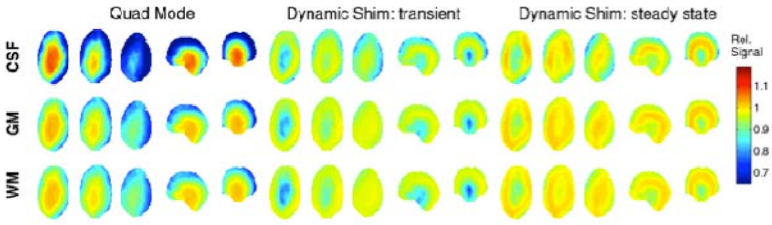

Fig 2: Simulated steady-state signals in 3 axial, 1 sagittal and 1 coronal plane. Signals are scaled relative to the ideal case for that tissue with no inhomogeneity

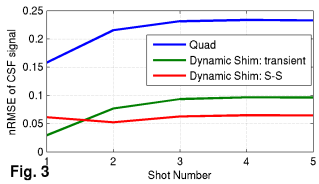

Fig. 3

Results & Discussion Figure 1b shows optimized pulse amplitudes/phases for the steady-state optimization (colours represent different transmit channels). Figure 2 depicts steady-state signals in the brain. Quad mode (standard) imaging results in large-scale variation of signal; this is alleviated by dynamic shimming of the transient response but there are still some areas of low signal, particularly in the centre of the brain. These are further improved by the steady-state optimisation which takes advantage of the "flip-up" pulses at the end of the shot to influence the ensuing steady state. Fig 3 shows the RMS difference between predicted CSF signal and the homogeneous case, as it evolves over 5 shots. The transient solution starts with the lowest error but this rises after multiple shots; the steady-state solution is better after a few shots. The errors are stable after 5 shots, justifying the use of Nshots=5 for optimization.

Conclusion Dynamic shimming with SR-EPG introduced the ability to design sequences of pulses together. In this work, the steady-state rather than transient behaviour of sequences is explicitly modelled and optimized, allowing more degrees of freedom and bringing us a step closer to directly controlling real signals resulting from imaging sequences.

References [1] Ibrahim et al, MRM 2001 19:1339 [2] Malik SJ et al, MRM 2012 68:1481 [3] Malik SJ, Proc ISMRM 2012:69 [4] Mugler JP et al, Proc ISMRM 2000:687 [5] Hennig J, JMR 1988 78:397 [6] Zelinka I & Lampinen J, Proc Intl Conf Soft Comp. 2000:177 [7] Alexander D, MRM 2008 60:439 [8] Yarnykh VL, MRM 2007 57:192 [9] Vernickel P et al, MRM 2007 58:381 [10] Van Uijen & den Boef MRM 1984 1:502